A Diffraction Study of Amorphous $Si_{0.40}C_{0.24}N_{0.36}$

H. Uhlig*, M. Frieß‡, J. Dürr, R. Bellissent**, H.-P. Lamparter, F. Aldinger, and S. Steeb

Max-Planck-Institut für Metallforschung, Institut für Werkstoffwissenschaft,
Seestraße 92 , 70174 Stuttgart, Germany

Z. Naturforsch. **51 a,** 1179–1184 (1996); received September 19, 1996

In the present work, amorphous $Si_{0.40}C_{0.24}N_{0.36}$ samples were investigated. X-ray and neutron diffraction experiments were performed, in order to evaluate the structure factors by the method of contrast variation. The structure can be described as crosslinked Si-N-C matrices. Within these matrices SiN_4 tetrahedra are predominant. Direct Si-Si contact does not occur. We report on the short range order and the nature of chemical bonding.

1. Introduction

Amorphous $Si_{0.40}C_{0.24}N_{0.36}$ samples were prepared from a commercial product (NCP 200, Chisso Corporation Japan). NCP 200 is a polyhydromethylsilazane with formula $[(CH_3)_2SiNH]_x[CH_3SiHNH]_y[CH_3SiN]_z$, with $x \approx y+z \approx 0.5$ [1]. The polymer consists of silazane-rings connected via Si-N- bonds with an average molecular weight of 1100 g/mol. This material is used as an organometallic precursor for Si-C-N ceramics, which show high crystallisation temperatures [1]. Conventional Si_3N_4 ceramics and composites of Si_3N_4 and SiC need metal-oxides as sintering aids, which are reducing the high temperature stability and the resistance towards corrosion. The material reported in this work is free of sintering additives and therefore provides good mechanical properties at high temperatures. A rigid, three dimensional network is formed in the amorphous state with high covalent character. Therefore the work in this paper focuses on the structure of the amorphous state, which is stable up to 1450°C. To describe the structure of the amorphous state, X-ray and neutron diffraction experiments yield valuable statistical information about the short range structure.

* Present Address: TU Chemnitz-Zwickau, Institute for Materials Research and Liquids, Reichenhainer Str. 70, 09107 Chemnitz

‡ Now with DLR Stuttgart, Institute for Structure and Design, Pfaffenwaldring 38 - 40, 70569 Stuttgart, Germany

** Laboratoire Léon Brillouin, CEA-CNRS Saclay, 91191 Gif-sur-Yvette cédex, France

Reprint requests to Dr. H. Uhlig.

2. Theoretical Background

From the coherently scattered intensity $I_{\mathrm{coh}}^{\mathrm{atom}}(Q)$, the total structure factor according to Faber and Ziman is obtained [2]:

$$S(Q)^{\mathrm{FZ}} = \frac{I_{\mathrm{coh}}^{\mathrm{atom}}(Q) - [\langle f(Q)^2\rangle - \langle f(Q)\rangle^2]}{\langle f(Q)\rangle^2}, \quad (1)$$

where:

$I_{\mathrm{coh}}^{\mathrm{atom}}(Q)$ = coherently scattered intensity per atom,

$\langle f(Q)^2\rangle = \sum_{i=1}^{n} c_i \cdot f_i(Q)^2$,

$\langle f(Q)\rangle = \sum_{i=1}^{n} c_i \cdot f_i(Q)$,

c_i = atomic concentration of atomic species i,

$f_i(Q)$ = atomic scattering length of atomic species i,

n = number of atomic species in the sample,

$Q = \frac{4\pi \sin(\theta)}{\lambda}$.

Fourier transformation of the total structure factor $S(Q)$ leads to the total pair distribution function $g(R)$:

$$g(R) = 1 + \frac{1}{4\pi\rho_0} \int_0^\infty Q^2[S(Q) - 1]\frac{\sin QR}{QR}\,\mathrm{d}Q \quad (2)$$

0932-0784 / 96 / 1200-1179 $ 06.00 © – Verlag der Zeitschrift für Naturforschung, D-72072 Tübingen

The total structure factor is the weighted sum of the partial structure factors $S_{ij}^{FZ}(Q)$, which describe the contribution of ij pairs to the total structure factor:

$$S(Q) = \frac{1}{\langle f \rangle^2} \sum_{i=1}^{n} \sum_{j=1}^{n} c_i c_j \cdot f_i f_j \cdot S_{ij}(Q). \quad (3)$$

The partial structure factors $S_{ij}(Q)$ lead to partial pair distribution functions $g_{ij}(R)$ by Fourier transformation. In general $S_{ij}(Q)$ are the unknown functions, so (3) leads to a simultaneous system of equations. In case of binary substances, three independent experiments, which differ in scattering lengths, are needed to solve the system of equations. In the case of ternary substances, six independent experiments are required to solve (3). The isotopic substitution of silicon and carbon would not lead to sufficient contrast in coherent scattering lenghts. The most promising candidate for isotopic substitution is nitrogen. But this is not applicable here because the polymer is produced during a commercial process.

Since six experiments are not possible in the present case, additional information is needed, e. g. by considering atomic distances known from crystalline compounds. Contrast variation concerning the Si and N atoms can be achieved by combination of X-ray diffraction and neutron diffraction.

3. Experimental

3.1. Samples

In order to yield ceramic monoliths which are required for the diffraction experiments by means of a newly developed polymer powder processing routline [1], the fusible and soluble polyhydromethylsilazane (NCP200) has to be crosslinked to a degree at which it can be ceramized without melting. This is induced by a thermal treatment at 400°C for 2 hours under flowing argon, yielding a colorless foam. The remaining fraction of lightweight oligomer is removed in vacuum ($5 \cdot 10^{-5}$mbar) within 1 hour at this temperature. The resulting polisilazane foam is milled for 30 min in a planetary mill using ZrO_2 balls and sieved through a 28 µm screen yielding a colorless polisilazane powder.

The powder is filled into rubber moulds and cold-isostatically pressed at 625 MPa yielding the desired shape. The polymer powder compact is then pyrolyzed in a quartz glass tube at a slow heating rate of 0.5 K/min to 1000°C under flowing argon. In the pyrolysis process the polymer powder compact is transformed into a black silicon carbonitride ceramic ($Si_{3+x}C_{x+y}N_4$) with a linear shrinkage of 28%. The given shape, however, is retained without any cracks. The obtained carbonitride is amorphous to X-rays with heat treatment up to temperatures of 1400°C in nitrogen atmosphere after a long holding of 50 hours when crystallization of α-Si_3N_4 occurs. At temperatures exceeding 1450°C at 1bar N_2-pressure the excess carbon (y C) reacts with Si_3N_4 to form SiC and N_2. The resulting ceramic is a Si_3N_4/SiC micro-nanocomposite [3].

For the X-ray diffraction experiments the samples obtained at 1000°C under argon were cut into 500 µm discs by a diamond wire saw and grinded by a diamond wheel in order to yield a smooth surface.

3.2. Diffraction Experiments

X-ray diffraction with amorphous $Si_{0.40}C_{0.24}N_{0.36}$ was done in transmission mode using Mo K_α radiation with a monochromator in the incident beam. The scattered intensity was detected using a position sensitive detector.

As $Si_{0.40}C_{0.24}N_{0.36}$ is a poor scatterer for X-rays, a measuring time of about 3 days was necessary to obtain sufficient counting statistics.

The sample for neutron diffraction was crushed into a coarse powder and put into a vanadium container. Neutron diffraction was done at LLB, Saclay, France using the instrument 7C2 at a wavelength of 0.703 Å.

In contrast to the X-ray experiments, $Si_{0.40}C_{0.24}N_{0.36}$ is a good scatterer for neutrons, thus a run of 4 hours yielded good results.

4. Results

4.1. Total Structure Factors

Figure 1 shows the total structure factor of X-ray diffraction. It displays a first maximum at 2.62 $Å^{-1}$ and a second maximum at 4.67 $Å^{-1}$. Beginning with 6.7 $Å^{-1}$ and ending at 9.2 $Å^{-1}$ a plateau region is formed by several overlaying broad maxima.

In Fig. 2, the raw data of the neutron scattering experiment are presented. The curve exhibits a small angle scattering effect at angles up to 10°. This could be a result of micropores which are formed during pyrolysis.

Regarding the curve along the entire 2Θ-range, a continuous decrease of scattered intensity is observed.

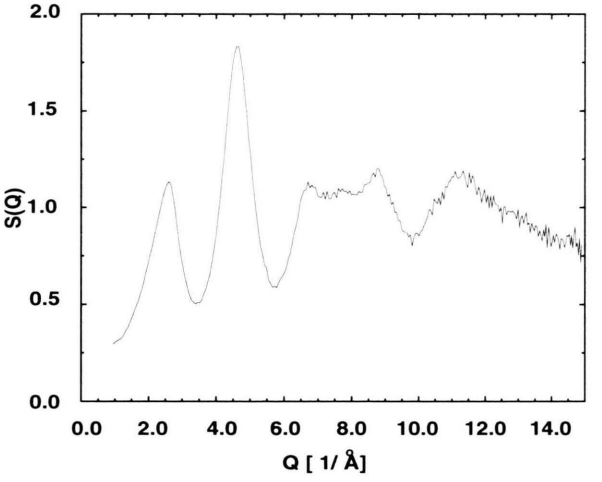

Fig. 1. Amorphous $Si_{0.40}C_{0.24}N_{0.36}$; X-ray diffraction (Mo-$K_\alpha$); total structure factor $S(Q)$.

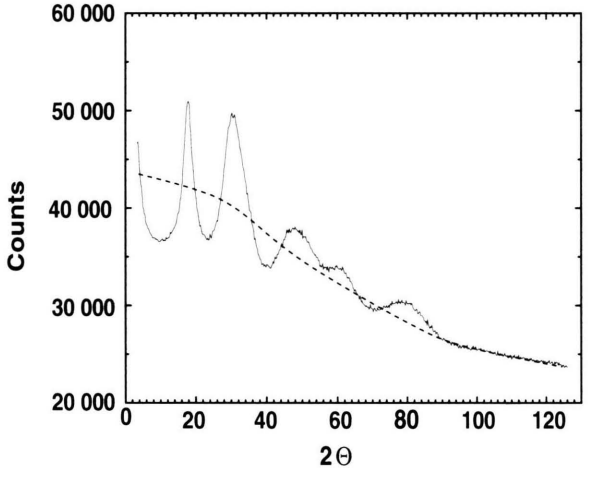

Fig. 2. Amorphous $Si_{0.40}C_{0.24}N_{0.36}$; Neutron diffraction, λ = 0.703 Å; raw data.

This indicates that the measured intensity contains a share of inelastically scattered intensity, which can not be removed using a two axis diffractometer. The origin of this rather high contribution results from the inelastic incoherent scattering of hydrogen corresponding to its incoherent scattering cross section, compared to most elements, and its small mass. The content of hydrogen could be estimated to amount to 7 at%. Therefore, the scattering data are corrected for inelastic scattering using the procedure described in [4]. Figure 3 shows the total structure factor after correction for absorption as well as for inelastic scattering.

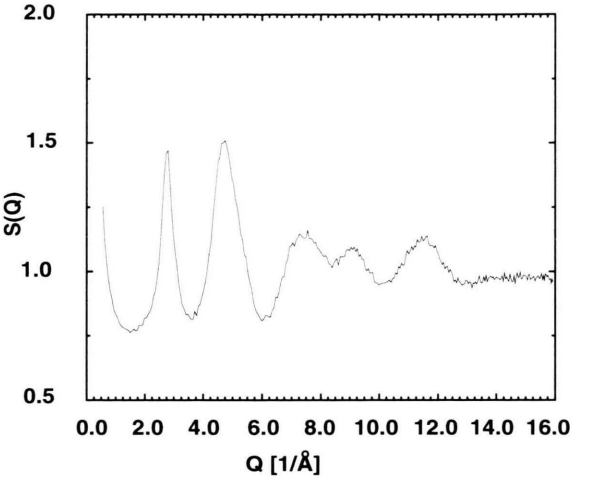

Fig. 3. Amorphous $Si_{0.40}C_{0.24}N_{0.36}$; Neutron diffraction; total structure factor $S(Q)$.

Two pronounced maxima are visible at 2.82 $Å^{-1}$ and 4.72 $Å^{-1}$.

4.2. Total Pair Distribution Functions

The straightforward application of (2) leads to truncation errors, particularly at low R-values. Therefore the kernel of (2) was multiplied with a window function.

$$F(Q) = \frac{1}{\sqrt{2\pi}} \exp(-\frac{1}{2} Q^2/\kappa^2) \qquad (4)$$

with κ = Gaussian parameter (κ = 0.12 $Å^{-1}$).

In order to explain the method of contrast variation using the two different sources of radiation, in Table 1 the weighting factors of the partial $g_{ij}(R)$ are presented.

The value of a certain weighting factor should exceed 0.1 in order to be able to recognize the corresponding pair correlation in the total distribution function. In case of X-ray diffraction Si-Si and Si-N correlations prevail the total pair distribution function.

Table 1. Amorphous $Si_{0.40}C_{0.24}N_{0.36}$. Weighting factors $c_i c_j f_i f_j / \langle f \rangle^2$ of the partial structure factors $S(Q)$.

	Pair $_{ij}$					
Method	Si–Si	Si–N	Si–C	N–N	N–C	C–C
X-ray	0.347	0.313	0.172	0.070	0.077	0.021
Neutron	0.064	0.259	0.118	0.264	0.240	0.055

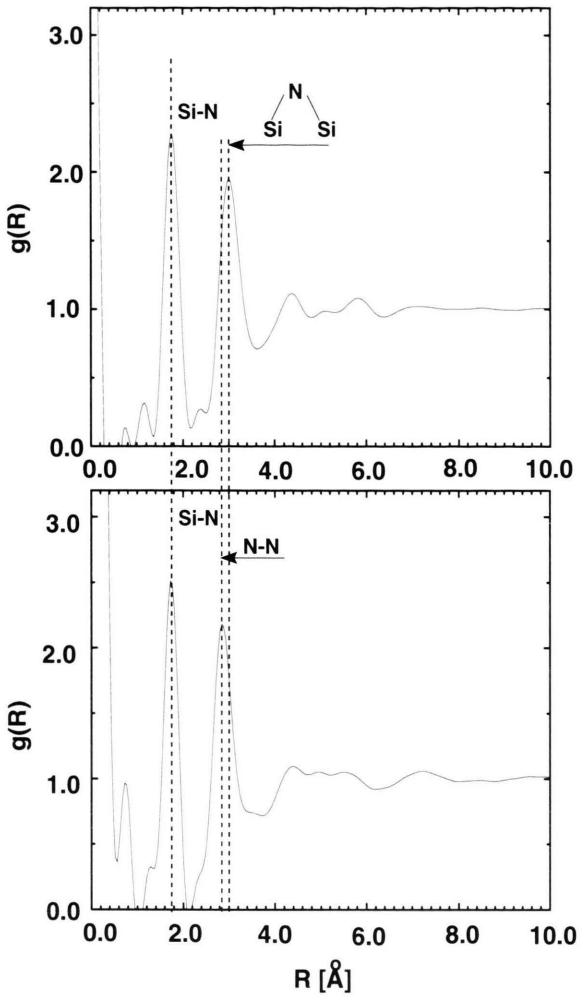

Fig. 4. Amorphous $Si_{0.40}C_{0.24}N_{0.36}$; total pair distribution functions g(R); X-ray diffraction (upper curve), Neutron diffraction (lower curve).

Si-C correlations should also be visible in the function. N-N, N-C, and C-C correlations have weighting factors below the threshold of visibility.

Due to the rather large coherent scattering length of nitrogen ($0.930 \cdot 10^{-12}$cm), N-N, N-C, and Si-N correlations give the main contribution to the total pair distribution function in the case of neutron radiation. The weighting factor of Si-C correlations is around the limit of visibility. Si-Si as well as C-C correlations are not expected to be seen in the total pair distribution function.

The total pair distribution functions in Fig. 4 show a rather similar run. This is not easy to understand, keeping in mind that the weighting factors differ essentially. The first peak of both curves can be associated with the Si-N bonds around 1.75 Å. This value is typical for crystalline Si-N compounds such as α-Si_3N_4 (1.715 Å to 1.759 Å) and β-Si_3N_4 (1.704 Å to 1.767 Å) [5].

According to Table 1, the maximum at about 3.0 Å of the X-ray pair distribution function is considered to be a mixture of higher Si-Si and higher Si-N correlations. Direct Si-Si contact would be expected at 2.43 Å and should be visible in the X-ray curve. This distance falls within a minimum of the pair distribution function, therefore direct Si-Si contact does not occur. The small ripple at 2.35 Å is a remainder of the truncation effect. In case of neutron diffraction, the situation becomes even more complicated regarding Table 1. The rather high value of the weighting factor for N-N bonds shifts the second maximum to lower R-values. In case of α/β-Si_3N_4, the N-N bond length is located at 2.82 Å. Using the first Si-N distance of 1.74 Å and the N-N distance of 2.82 Å, the average N-Si-N bond angle can be calculated to 108.26°, which is equivalent to the ideal tetrahedron angle of 109.25° within the experimental error. Higher correlations, which are present at 4.0 Å up to 8.0 Å, cannot be related to certain pair correlations.

Table 2. Amorphous $Si_{0.40}C_{0.24}N_{0.36}$. Position of the first maximum of $g(R)$.

Method	Si–N Peak Position [Å]	Half Width [Å]	Height	Coordination Number
X-Ray	1.76±0.02	0.38	2.28	3.3±0.4
Neutron	1.74±0.02	0.36	2.52	3.9±0.4

The existence of Si-C correlations needs a detailed discussion of the first maximum. The data of Table 2 were used to fit Gaussian curves to the total distribution functions $g(R)$. This procedure is presented in Figure 5.

Under the assumption that this first maximum is formed by Si-N correlations only, the partial coordination number Z_{SiN} as given in Table 2 can be calculated from the peak area N_{ij} using the equation

$$Z_{ij} = N_{ij} \cdot \frac{\langle f \rangle^2}{c_i c_j f_i f_j} \cdot c_j. \tag{5}$$

Regarding Fig. 5, it is obvious, that the insertion of further Gaussian curves is limited. The number of

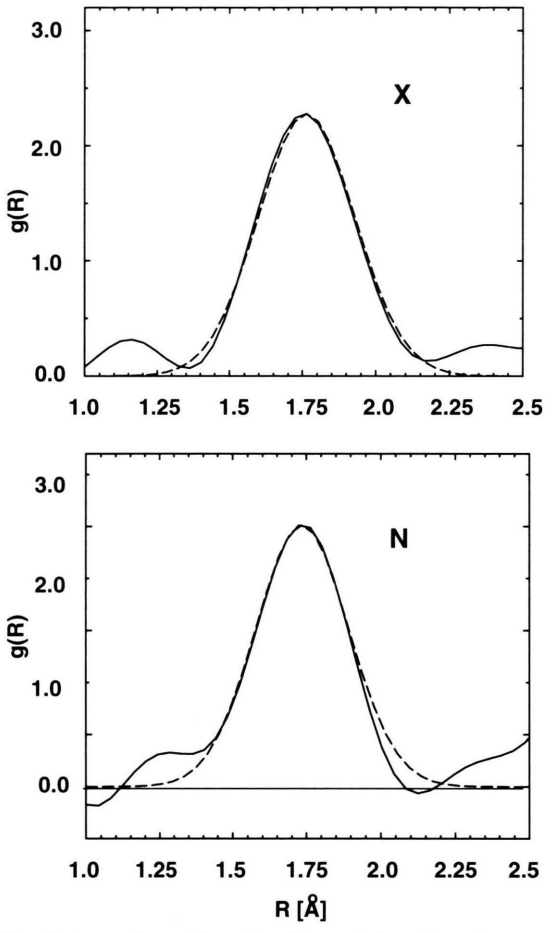

Fig. 5. Amorphous $Si_{0.40}C_{0.24}N_{0.36}$; fitting Gaussian curves to total pair distribution functions.

Si-C bonds at their corresponding length near 1.9 Å [6] can only be small compared to the Si-N bonds.

This means that the number of existing Si-C bonds in the material, if occuring at all, is rather low, compared to that of Si-N.

Due to the low values of the weighting factors of the C-C correlations in both experiments, the question of the chemical bonds of carbon cannot be discussed in the present paper.

5. Discussion

In this paper, the total pair correlation functions of $Si_{0.40}C_{0.24}N_{0.36}$ are presented. The paper [7] reports on several amorphous $Si_xC_yN_z$ compositions. The present paper extends this study to higher silicon content but rather low nitrogen content. Anyway, the discussion here must include studies of amorphous Si_3N_4[8], crystalline-SiC [6], and amorphous carbon [9].

In Table 3, the peak positions of the first and following maxima of the pair distribution functions derived from the neutron diffraction experiments are listed.

The pair distribution function of amorphous $Si_{0.40}C_{0.24}N_{0.36}$ shows a rather similar run to that of amorphous Si_3N_4 as reported in [8].

The absence of any peak at 3.62 Å is an additional proof for absence of substantial Si-C bonds. The small ripple at 1.3 Å might be a signal from C=N bonds but is more likely due to a truncation effect caused by the Fourier transformation.

The strong similarity of the pair distribution functions of amorphous $Si_{0.40}C_{0.24}N_{0.36}$ and of amorphous Si_3N_4 leads to the question of the arrangement of the C-atoms. The value of the weighting factor of C-C correlations in our case is too small to answer that question straightforwardly. To address this question, two models can be discussed. The first model is, that phase separation at an early stage during sample preparation took place. In that case amorphous carbon is segregated from an amorphous Si_3N_4 matrix by forming small carbon-rich segregations. Carbon rich segregation is also suggested by the small angle intensity observed here. The second idea is that carbon is distributed homogeneously over the whole body, not prefering or avoiding any certain kind of chemical bond. This could be a reason for detecting Si-C bonds in NMR-experiments [10].

In [11] the structure of amorphous $Si_{0.28}C_{0.42}N_{0.28}$ with 0.02 at% oxygen impurity is reported. The authors propose an amorphous silicon-carbonitride

Table 3. Amorphous $Si_{0.40}C_{0.24}N_{0.36}$, Position of the peaks of $g(R)$; neutron diffraction.

Compound	Ref.	Peak position [Å]											
amorphous $Si_{0.40}C_{0.24}N_{0.36}$			1.74		2.84		4.34	4.97	5.63				7.22
amorphous Si_3N_4	[8]		1.75		3.0	(3.5)	4.3	4.9	5.8				7.1
c-SiC	[6]		1.89		(3.0)	3.62	4.37	4.7	5.4				
amorphous Carbon	[9]	1.53		2.4		3.8	(4.3)	4.9	5.8	6.2	6.9		7.1

phase $Si_{1.0}N_{0.98}C_{0.35}$ coexisting with 1.25 free carbon in the sample. They also report about a hydrogen content of the annealed material.

Material annealed at 1200°C for 1 hour contains 19 at% hydrogen, material annealed at 1400° for the same time indicates 5 at% hydrogen, and elongated annealing for 6 hours at 1400°C indicates 0.3 at% hydrogen. All together, hydrogen is not removed completely under the conditions employed above. This leads to the idea that the Si-atoms are not saturated completely by four neighbouring N or C atoms. Also Si-H bonds and even free Si-bonds, forming so-called dangling bonds into inner surfaces induced by micropores have to be taken into account. Due to the low concentration of H and its low coherent scattering length of about $-0.37 \cdot 10^{-12}$cm H-bonds are not visible in the total pair distribution function. Hydrogen content and free Si-dangling bonds forming micropores of several Å in diameter can serve as an explanation of the Si-N coordination being smaller than four as reported in this paper, Table 2. Again, these micropores contribute to the small angle intensity.

6. Conclusion

Amorphous $Si_{0.40}C_{0.24}N_{0.36}$ samples have been investigated by X-ray and neutron diffraction experiments. The pair distribution functions indicate a rather similar structure to amorphous Si_3N_4. A highly connected three dimensional Si-N network can be proposed as a model for amorphous $Si_{0.40}C_{0.24}N_{0.36}$. With the experiments reported here it is not possible to clarify the structural environment of carbon atoms. To answer this question further studies, e. g. an EXAFS-study at the silicon K-edge or even the carbon K-edge, are proposed.

[1] R. Riedel, G. Passing, H. Schönfelder, and R. J. Brook; Nature **355**, 714 (1992).
[2] T. E. Faber and J. M. Ziman , Phil. Mag. **11**, 153 (1965).
[3] M. Frieß, J. Bill, F. Aldinger, D. V. Szabó and R. Riedel; Key Engineering Materials **89 - 91**, 95 (1994).
[4] D. Seyferth, G. Wiseman, J. Amer. Cer. Soc. **67**, C132 (1994); additional information: product information, Chisso corporation, Japan.
[5] W. G. Jung, M. D. Zeidler, and P. Chieux, Mol. Phys. **68(2)**, 473 (1989).
[6] S. N. Ruddleson and P. Popper, Acta Cryst. **11**, 465 (1958).
[7] P. T. B. Shaffer, Acta Cryst. **B25**, 477 (1969).
[8] J. Dixmier, P. Baudoin, R. Bellissent, A. M. Flank, H. Roulet, A. Georghiu, G. Dufour, C. Sénémaud, E. Musset, N. Herlin, and M. Cauchetier, Proc. Fourth Euroceramics, **1**, 233 (1994).
[9] T. Aiayma, T. Fukanaga, K. Niihara, T. Hirai, and K. Suzuki, Non. Cryst. Sol. **33**, 131 (979).
[10] P. H. Gaskell, in J. Zarzycky (editor), Materials Science and Technology **9**, 230 (1991), Verlag Chemie, Weinheim, Germany.
[11] J. Seitz, J. Bill, N. Egger, and F. Aldinger J. Eur. Ceram. Soc. **16**, 885 (1996).
[12] J. Dixmier, R. Bellissent, D. Bahloul, and P. Goursat, Eur. Ceram. Soc. **13**, 293 (1994).